PHYSICAL REVIEW C **81**, 061302(R) (2010)

Extreme nuclear shapes examined via giant dipole resonance lineshapes in hot light-mass systems

Deepak Pandit,[1] S. Mukhopadhyay,[1] Srijit Bhattacharya,[2] Surajit Pal,[1] A. De,[3] S. Bhattacharya,[1] C. Bhattacharya,[1] K. Banerjee,[1] S. Kundu,[1] T. K. Rana,[1] A. Dey,[1] G. Mukherjee,[1] T. Ghosh,[1] D. Gupta,[1,4] and S. R. Banerjee[1,*]

[1]*Variable Energy Cyclotron Centre, 1/AF-Bidhannagar, Kolkata-700064, India*

[2]*Department of Physics, Darjeeling Government College, Darjeeling-734101, India*

[3]*Department of Physics, Raniganj Girls' College, Raniganj-713358, India*

[4]*Bose Institute, Department of Physics and Centre for Astrophysics and Space Science, Salt Lake City, Kolkata-700091, India*

(Received 17 February 2010; revised manuscript received 26 May 2010; published 16 June 2010)

The influence of α clustering on nuclear reaction dynamics is investigated using the giant dipole resonance (GDR) lineshape studies in the reactions ^{20}Ne ($E_{\rm lab}$ = 145, 160 MeV) + ^{12}C and ^{20}Ne ($E_{\rm lab}$ = 160 MeV) + ^{27}Al, populating ^{32}S and ^{47}V, respectively. The GDR lineshapes from the two systems are remarkably different from each other. Whereas, the non-α-like ^{47}V undergoes Jacobi shape transition and matches exceptionally well with the theoretical GDR lineshape estimated under the framework rotating liquid drop model (RLDM) and thermal shape fluctuation model (TSFM) signifying shape equilibration, for the α cluster ^{32}S an extended prolate kind of shape is observed. This unusual deformation, seen directly via γ decay for the first time, is predicted to be due to the formation of orbiting dinuclear configuration or molecular structure of ^{16}O + ^{16}O in the ^{32}S superdeformed band.

DOI: 10.1103/PhysRevC.81.061302 PACS number(s): 24.30.Cz, 24.60.Dr, 25.70.Gh

In recent years, there have been intense theoretical and experimental efforts [1,2] to search for highly (super/hyper)deformed (SD/HD) nuclear systems. There are indications that such highly deformed shapes are likely to be observed in light α-like systems ($A_{CN} \sim$ 20–60) at higher angular momenta (typically, $\gtrsim 15\hbar$) and excitation energies (typically, $\gtrsim$ 40 MeV). Experimentally, large deformations were observed in ^{36}Ar [3]and ^{40}Ca [4], where the deformations were studied using γ-spectroscopic techniques. In recent times, experimental indications of hyperdeformation have also been reported in the decay of ^{56}Ni [5,6] and ^{60}Zn [7], where charged particle spectroscopy was used to identify the ternary fission-like decay of hyperdeformed composites. Hyperdeformed shape in ^{36}Ar has also been predicted [8], however, it is not yet firmly established experimentally [1].

Such large deformations observed in light α-like systems are believed to be due to the occurrence of either quasimolecular resonances or nuclear orbiting [9], which have the origin in α-cluster structure of these nuclei. On the other hand, rapidly rotating light nuclei in general are likely to undergo Jacobi shape transition at an angular momentum value near the fission limit, where the shape changes abruptly from noncollective oblate to collective triaxial and/or prolate shape. Since it is possible for the light mass nuclei to attain very high angular velocities beyond the critical point for Jacobi transition without undergoing fission, existence of exotic shapes in nuclei with a large deformation becomes likely. Signatures of such shape transitions in ^{45}Sc [10] and ^{46}Ti [11–13] have been reported from the study of line shapes of giant dipole resonance (GDR) built on excited states. Recently, the Jacobi shape transition has been confirmed for ^{48}Cr [14] from high-spin spectroscopy and corresponding theoretical calculation using the LSD liquid drop model [15]. It is, therefore, relevant to explore the relationship between the shapes of the light α-like systems and the corresponding Jacobi shapes, which would help in understanding the reaction dynamics of light α-like systems and the role played by α-clustering in determining the shape.

The aim of the present study is to make quantitative experimental estimation of the deformed shapes of light α and non-α systems using GDR lineshape studies and compare them with the corresponding predictions for equilibrium Jacobi shapes. For the α-like system, we have taken ^{20}Ne + ^{12}C system and for a non-α-like system, we have chosen ^{20}Ne + ^{27}Al system. The ^{20}Ne + ^{12}C system is a well-established orbiting system [16], and our previous studies on enhancement of fragment yield near the entrance channel [17] as well as α-spectroscopic studies [18] have strongly indicated a highly deformed orbiting dinuclear shape for this system. On the contrary, for non-α-like ^{47}V system, it is well established that there is no significant entrance channel effect and fusion-fission compound nuclear yield is dominant in accordance with the qualitative expectation from the number of open channels model [19,20]. Since α-spectroscopic studies can only indicate effective deformation in an indirect way, it is worthwhile to complement the above studies with the investigation of nuclear shapes of the excited rotating systems through the GDR γ decays in a more direct manner.

The GDR, linear oscillations of the protons and neutrons in the hot nucleus, occurs on a time scale that is sufficiently short. Thus, these can compete with other modes of nuclear decay. In addition, the resonance couples directly with the other nuclear degrees of freedom, such as shape degrees of freedom, and thus can provide information on the shape evolution of the nuclei at finite temperature and fast rotation. The resonance energy being proportional to the inverse of the nuclear radius, the GDR strength function splits in the case of deformed nuclei and the investigation of the strength distribution gives a direct access to nuclear deformations. Here, we report the experimental GDR strength functions for the hot, rotating composites formed in

*srb@veccal.ernet.in

^{20}Ne + ^{12}C and ^{20}Ne + ^{27}Al systems and show, that, whereas the experimentally extracted shape for ^{20}Ne + ^{27}Al conforms to the predicted Jacobi shape, extracted shape of the ^{20}Ne + ^{12}C system is highly elongated (prolate) and does not conform to the corresponding Jacobi shape, clearly highlighting the difference between the reaction mechanisms in the two cases.

The ^{47}V and ^{32}S nuclei were formed by bombarding pure 1 mg/cm^2 thick ^{27}Al and ^{12}C targets with accelerated ^{20}Ne beams from the K-130 cyclotron at the Variable Energy Cyclotron Centre, Kolkata, India. The initial excitation energy for ^{47}V compound system was $E_x = 108$ MeV corresponding to a projectile energy $E_{\rm proj} = 160$ MeV. Similarly the initial excitation energies for ^{32}S nucleus were $E_x = 73$ and 78 MeV corresponding to the projectile energies of $E_{\rm proj} = 145$ and 160 MeV. The corresponding critical angular momenta for ^{47}V and ^{32}S nuclei are $l_{cr} = 38\hbar$ and $24\hbar$, respectively, the same as those extracted from the previous complete fusion measurement by using the sharp cut-off approximation for ^{47}V [21] and ^{32}S [22]. These values extend well beyond the critical angular momentum values of $29.6\hbar$ and $21.5\hbar$ at which the Jacobi transitions are predicted to occur for these nuclei (according to systematics $J_c = 1.2A^{5/6}$ [23]). They are formed in identical conditions as in the previous charged particle experiment reported earlier [18]. The experimental arrangement and technique was similar to that described earlier [24]. The high energy photons were detected at $\theta_\gamma = 55^\circ$ with a part of the LAMBDA (Large Area Modular BaF_2 Detector Array) spectrometer arranged in a 7 × 7 square matrix [25]. An event-by-event information of the populated angular momentum was recorded using a 50 element BaF_2 based low energy γ-multiplicity filter in coincidence with the high energy photon events. The multiplicity filter was kept at a distance of 10 cm from the target which ensured the selection of higher part of the spin distribution. The schematic view of the experimental setup is shown in Fig. 1. A time of flight (TOF) technique was used to eliminate neutrons while the pulse shape discrimination (PSD) was adopted to reject pile-up events for the individual detector elements. The PSD and the TOF spectra for a single detector are shown in Fig. 2 clearly indicating an excellent rejection of neutrons and pile-up events.

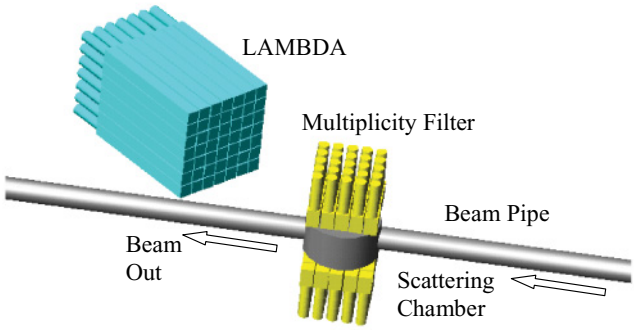

FIG. 1. (Color online) Schematic view of experimental setup for the LAMBDA (Large BaF2 Array) spectrometer in a 7 × 7 matrix arrangement along with the low energy γ-ray multiplicity filter.

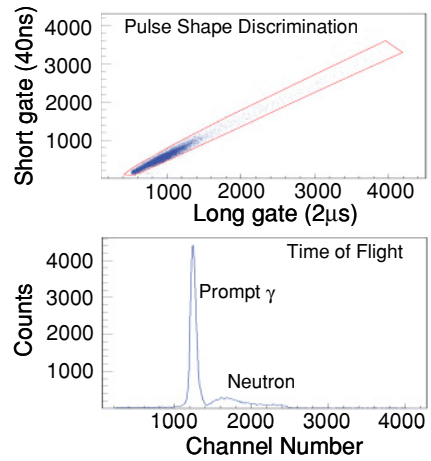

FIG. 2. (Color online) The experimental pulse shape discrimination and time-of-flight spectra obtained from a single detector.

The linearized GDR spectra from ^{47}V (for two angular momentum windows) and ^{32}S (for two incident energies) are shown in Fig. 3. The GDR lineshapes from the two systems are remarkably different, from which one usually gets in the case of a spherical or a near spherical system and indicate large deformations. The most striking feature in the case of ^{47}V populated at $28\hbar$ and $31\hbar$ is the strong enhancement in the γ yield at ∼10 MeV similar to one observed in ^{46}Ti [11] earlier. It is characteristic of a large deformation and the effect

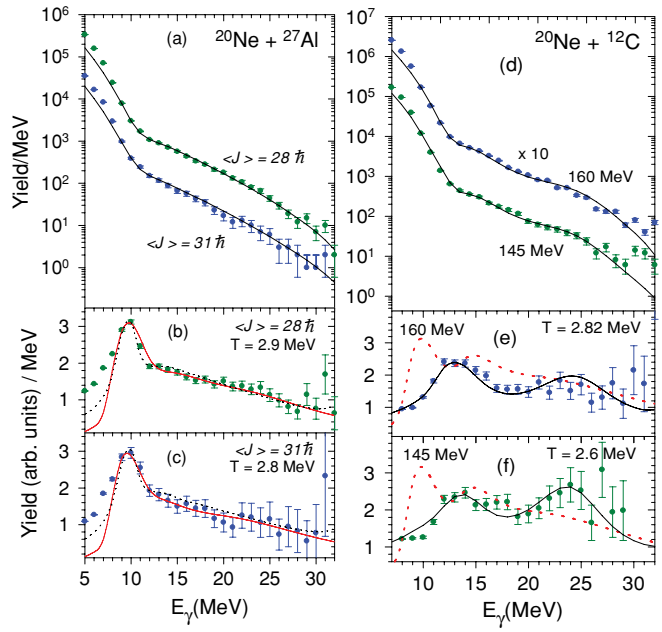

FIG. 3. (Color online) (a) The experimental γ-spectra and extracted linearized GDR strength functions (b),(c) for ^{47}V for the two angular momentum windows. The dotted lines are the respective CASCADE predictions and the solid lines are the predicted line shapes from the free energy minimization technique. Same for ^{32}S for two incident energies (d),(e),(f). The solid lines are the CASCADE predictions using 2-GDR components and the dotted lines are the predicted line shape from the free energy calculations.

TABLE I. Extracted GDR parameters for ^{32}S used for CASCADE calculations. E_1, E_2, Γ_1, Γ_2, S_1, S_2 are the resonance energies, widths, and fractional strengths, respectively, for the two GDR components.

E_{proj} (MeV)	E_1 (MeV)	Γ_1 (MeV)	S_1	E_2 (MeV)	Γ_2 (MeV)	S_2	β
145	14.5	6.2	0.37	25.4	7.5	0.63	0.68
160	14.0	6.2	0.32	26.0	8.2	0.68	0.76

of coriolis splitting due to very high angular velocity in the system. Such very high angular velocities are usually achieved by the system normally beyond the Jacobi transition point. However, for ^{32}S no such enhancement is seen though the nucleus is populated at spins well beyond Jacobi transition point. A two-component GDR strength function fits the experimental data fairly well. The extracted parameters are given in Table I. The shape looks more like a highly extended prolate and is seen for the first time for this nucleus. The GDR lineshape for ^{47}V, on the other hand, is more complex and a simple two or three component GDR strength function fails to describe the experimental observations. The linearized GDR lineshapes were extracted using a modified version of the statistical model code CASCADE [24,26]. For both the cases we have adopted the Ignatyuk level density prescription [27] keeping the asymptotic level density parameter $\tilde{a} = A/8$ MeV^{-1}. The CASCADE calculations have been performed with the same parameters as used in the charged particle analysis except for the $\delta 1$ parameter in the case ^{32}S. We have taken $\delta 1$ as 1.0×10^{-3} in order to explain the low energy part of the γ spectrum.

In order to interpret the extracted GDR strength functions in the entire γ-ray energy region (5–32 MeV) and to understand the equilibrium deformations in these hot and rotating nuclear systems, a calculation is performed for estimating the equilibrium shape of a nucleus by minimizing the total free energy under the framework of rotating liquid drop model (RLDM) and thermal shape fluctuation model (TSFM) for a given temperature T and angular momentum J. Earlier, a similar model with a modified liquid drop parametrization (LSD model) was used to extract the shape evolution of ^{46}Ti and ^{48}Cr [11,14,15].

The free energy for a hot rotating nucleus at a constant spin (J), in a liquid drop picture, can be written as [28]

$$F(T, J, \beta, \gamma) = E_{\text{LDM}}(\beta, \gamma) - TS + \frac{J(J+1)\hbar^2}{2(\omega \cdot I \cdot \omega)}, \qquad (1)$$

where

$$\omega \cdot I \cdot \omega = I_{xx} \sin^2\theta \cos^2\phi + I_{yy} \sin^2\theta \sin^2\phi + I_{zz} \cos^2\theta$$

is the moment of inertia about the rotation axis ω. I_{xx}, I_{yy}, I_{zz} are the principal rigid body moments of inertia and S is the entropy of the system. The dependence of level densities on deformation and shell corrections are assumed to be small and neglected as the nuclear temperatures in this case are $\sim$3 MeV. $E_{\text{LDM}}(\beta,\gamma)$ is the deformed liquid drop energy, calculated in terms of β and γ, the intrinsic quadrupole deformation parameters [29–32]. The deformed moment of inertia can be written in the Hill-Wheeler parametrization as $I_{zz} = B_1 \frac{2}{5} m r_0^2 A^{5/3}$, where, $B_1 = \frac{1}{2}(r_1^2 + r_2^2)$, $r_1 = R_x/R_0 = \exp(\sqrt{5/4\pi})\beta \cos(\gamma - 2\pi/3)$ and, $r_2 = R_y/R_0 = \exp(\sqrt{5/4\pi})\beta \cos(\gamma + 2\pi/3)$. R_x, R_y are the deformed radius parameters along the directions perpendicular to the spin axis and R_0 is that for an equivalent undeformed spherical shape. We have considered rotation axis along z, different from the common convention of ω as parallel to x, as it leads to simplification of many expressions and calculations. However, we have plotted γ as $(\gamma - 120^\circ)$ in Figs. 4 and 5 in order to represent the equilibrium deformation in the conventional way.

The free energy surfaces were obtained for different spins over the entire β-γ space as shown in Fig. 4 for ^{47}V compound nucleus. It can be clearly seen that as the spin increases, the minima of the free energy surfaces move toward increasing oblate deformation (along the y-axis) and suddenly make a transition toward the prolate ($\gamma = 0^\circ$) deformation (represented by the line) at high spins. The gradual evolution in shape and the transition point are evident in a polar β vs γ plot for discrete spins (Fig. 5). It is clear from the figure that for ^{47}V, with the increase in angular velocity, the nucleus becomes more and more oblate deformed ($\gamma = 60^\circ$). After a critical spin of $27\hbar$ it suddenly becomes triaxial ($60^\circ < \gamma < 0^\circ$) and approaches a prolate shape at still higher spins.

Experimentally, the average angular momentum was deduced from a selection of the fold distribution of the low energy γ-multiplicity filter array [24] and corresponding

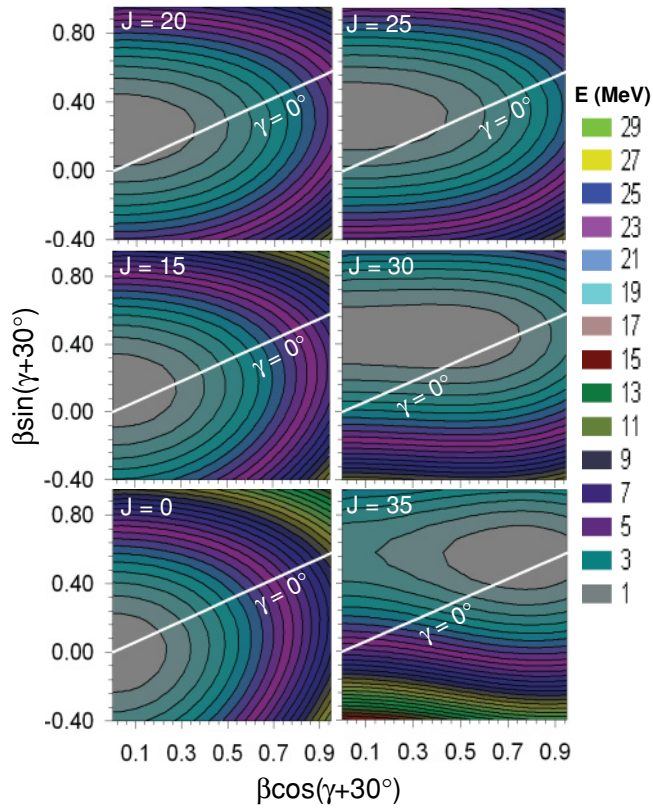

FIG. 4. (Color online) Liquid drop free energy surfaces at different spins for ^{47}V. The line represents the prolate shape ($\gamma = 0$).

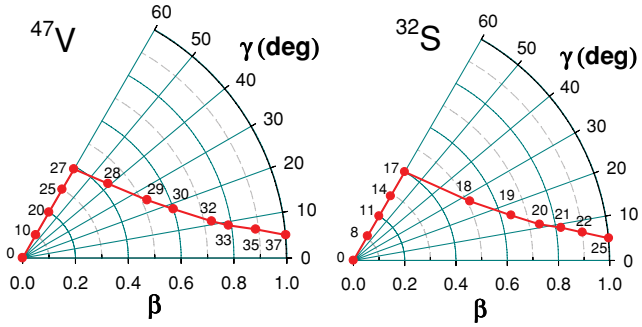

FIG. 5. (Color online) The equilibrium shapes are plotted as a function of quadrupole deformation parameters β and γ for different spins for ^{47}V and ^{32}S nuclei. The discrete spin values are represented alongside the data points.

to the $\langle J \rangle$ values the equilibrium shape of the nucleus is known (Fig. 5). The GDR observables ($E_{\rm GDR}$, $\Gamma_{\rm GDR}$) are built on these shapes using the Hill-Wheeler parametrization and considering $\Gamma^i_{\rm GDR} = \Gamma_0 (E^i_{\rm GDR}/E_0)^\delta$ [33], where, Γ_0 is the ground state GDR width and δ is taken as 1.9. This procedure in general gives three different GDR frequencies (along the three unequal axes) and widths corresponding to a particular angular momentum and equilibrium shape of the nucleus. These three GDR frequencies further split (the ones perpendicular to the spin axis) due to coriolis effect as the GDR vibrations in a nucleus couple with its rotation when viewed from a nonrotating frame [34]. The magnitude of the split depends on the magnitude of the rotation frequency and give rise to five GDR components. The resultant GDR lineshape is obtained as a superposition all the components (E_i, Γ_i),

$$\sigma_{\rm total} = \sum_{i=1}^{5} \frac{E_\gamma^2 \Gamma_i}{\left(E_\gamma^2 - E_i^2\right)^2 + E_\gamma^2 \Gamma_i^2}.$$

The TSFM assumes that at high T and J, the GDR vibration samples an ensemble of different shapes around the equilibrium shape of the compound nucleus. Thus, the GDR lineshapes are generated (according to the adiabatic TSFM [35]) by averaging the GDR vibrations over the free energy surfaces [using a Boltzman probability distribution $\exp(-F/T)$] in the entire deformation space including full orientation fluctuation using

$$\langle \sigma \rangle = \frac{\int D_\alpha e^{-F/T} (\omega \cdot I \cdot \omega)^{-3/2} \sigma}{\int D_\alpha e^{-F/T} (\omega \cdot I \cdot \omega)^{-3/2}},$$

where $D_\alpha = \beta^4 \sin(3\gamma)\, d\beta d\gamma d\Omega$ is the elemental volume.

The resultant lineshape is compared with the experimental data and is plotted in Fig. 3 (solid line). It describes the data for ^{47}V remarkably well for both the experimentally measured spin windows of $28\hbar$ and $31\hbar$ (spin uncertainties of $\pm 7\hbar$ & $\pm 8\hbar$, respectively) at corresponding temperatures of 2.9 and 2.8 MeV, respectively. The extracted GDR parameters are shown in Table II. The presence of the enhancement in the lineshape at $\sim$10 MeV and the goodness of description are

TABLE II. Calculated GDR parameters for ^{47}V from RLDM & TSFM calculations. E_i, Γ_i, S_i are the resonance energies, widths and fractional strengths respectively for the five GDR components after coriolis splitting.

$E_{\rm proj}$ (MeV)	$\langle J \rangle = 28\hbar$				$\langle J \rangle = 31\hbar$			
	E_i	Γ_i	S_i	β	E_i	Γ_i	S_i	β
160	9.9	3.0	0.33	0.43	9.9	3.0	0.33	0.67
	14.5	5.3	0.15		14.1	5.1	0.15	
	18.3	8.1	0.17		18.4	8.4	0.17	
	23.1	11.3	0.17		23.0	11.5	0.17	
	27.3	15.5	0.18		27.8	15.8	0.18	

characteristic signatures of Jacobi transition in the case of ^{47}V nucleus at these spin values.

Since it is difficult to extract the angular momentum for very low mass accurately, the ^{32}S nucleus was populated with two incident energies, 145 and 160 MeV, in order to populate ^{32}S at different spins. The high-fold gated spectrum of ^{32}S for both the energies is shown in Fig. 3. The similar free energy calculations are done at both low and high spins, but it fails miserably to describe the experimental data. The calculation performed at $22\hbar$ is shown in Fig. 3 [dotted line (e),(f)]. Though the nucleus is populated well above the critical spin for Jacobi transition (Fig. 5), it does not show the characteristic behavior of such a transition in shape. Instead, the data are reproduced quite well by a statistical model (CASCADE) calculation with a two-component GDR strength function (Table I). The shapes suggest a strongly prolate deformed nucleus ($\beta \approx 0.76$ for $E_{\rm proj} = 160$ MeV, corresponding to an axis ratio of 1.7:1). The ^{20}Ne + ^{12}C system was studied earlier at 5 MeV/nucleon and 9.5 MeV/nucleon to study the isospin effects in light mass nuclei [36] but only preliminary result was presented for the higher incident energy indicating toward incomplete fusion. Indeed, the pre-equilibrium component at 200 MeV incident energy, as measured from our earlier charge particle experiment, is around 50%. However, the pre-equilibrium component in our case, less than 10% for 160 MeV and negligible at 145 MeV, does not seem to have a major influence on the high energy γ spectra.

The occurrence of such a large deformation without showing the characteristics of Jacobi transition is possible only if some other reaction mechanism is responsible. One of the possibilities could be the formation of an orbiting dinuclear complex where the nucleus is not fully equilibrated (in terms of shape degrees of freedom) and maintains the entrance channel shape before finally splitting into two parts. Our charged particle studies have also indicated a highly deformed orbiting dinuclear shape of this system. However, it can also be conjectured that the observed unusual deformation can be due to the formation of the molecular structure of the ^{16}O + ^{16}O cluster in ^{32}S. In the theoretical work of Kimura and Horiuchi [37], it was predicted that the SD states of ^{32}S have considerable amount of ^{16}O + ^{16}O components and become more prominent as the excitation energy increases. The extracted deformation for two touching ^{16}O was found

to be $\beta = 0.73$ which is in agreement with the experimentally extracted deformation from the resonance energy peaks. The occurrence of GDR in nuclei, where the entire nucleus takes part in a collective manner, is clearly an effect of the mean field structure of the nucleus. It is also known that other inherent structures (molecular resonance and/or orbiting dinuclear complex) in light α-cluster nuclei may coexist with the mean field description of the nucleus. Whether the experimental signatures of the overall nuclear deformation via GDR γ decay is due to the coexistence of these effects needs to be investigated further and are beyond the scope of this present study.

In summary, we have populated the nuclei ^{47}V and ^{32}S at the highest spins and high excitations and studied their shapes directly by looking at the lineshapes of their GDR decay. Both the nuclei show highly deformed structures corresponding to highly fragmented GDR strength functions. The ^{47}V nucleus shows Jacobi triaxial shapes well beyond the critical transition point. The evolution of the nucleus as a function of angular momenta is estimated in the RLDM and TSFM framework and found to match exactly with the experiment. In the case of the α cluster ^{32}S nucleus, a highly deformed extended prolate configuration is evident which does not follow the usual evolution of shape with angular momentum. This unusual deformation, seen directly for the first time, can be speculated due to the formation of either the orbiting dinuclear configuration or molecular structure of $^{16}\mathrm{O} + {}^{16}\mathrm{O}$ in ^{32}S SD band.

[1] C. Beck *et al.*, Phys. Rev. C **80**, 034604 (2009), and references therein.
[2] C. Beck *et al.*, Int. J. Mod. Phys. E **17**, 2049 (2008).
[3] C. E. Svensson *et al.*, Phys. Rev. Lett. **85**, 2693 (2000).
[4] E. Ideguchi *et al.*, Phys. Rev. Lett. **87**, 222501 (2001).
[5] C. Wheldon *et al.*, Nucl. Phys. A **811**, 276 (2008).
[6] W. von Oertzen *et al.*, Eur. Phys. J. A **36**, 279 (2008).
[7] W. von Oertzen *et al.*, Phys. Rev. C **78**, 044615 (2008).
[8] A. Algora, J. Cseh, J. Darai, and P. O. Hess, Phys. Lett. B **639**, 451 (2006).
[9] S. J. Sanders, A. Szanto de Toledo, and C. Beck, Phys. Rep. **311**, 487 (1999).
[10] M. Kicihska-Habior *et al.*, Phys. Lett. B **308**, 225 (1993).
[11] A. Maj *et al.*, Nucl. Phys. A **731**, 319 (2004).
[12] M. Brekiesz *et al.*, Nucl. Phys. A **788**, 224c (2007).
[13] M. Kmiecik *et al.*, Acta Phys. Pol. B **38**, 1437 (2007).
[14] M. D. Salsac *et al.*, Nucl. Phys. A **801**, 1 (2008).
[15] K. Pomorski and J. Dudek, Phys. Rev. C **67**, 044316 (2003).
[16] D. Shapira, J. L. C. Ford, J. GomezdelCampo, R. G. Stokstad, and R. M. DeVries, Phys. Rev. Lett. **43**, 1781 (1979).
[17] C. Bhattacharya *et al.*, Phys. Rev. C **72**, 021601(R) (2005).
[18] Aparajita Dey *et al.*, Phys. Rev. C **74**, 044605 (2006).
[19] A. Ray *et al.*, Phys. Rev. C **44**, 514 (1991).
[20] C. Beck *et al.*, Phys. Rev. C **47**, 2093 (1993).
[21] Nguyen Van Sen, R. Darves-Blanc, J. C. Gondrand, and F. Merchez, Phys. Rev. C **27**, 194 (1983).
[22] F. Saint-Laurent *et al.*, Nucl. Phys. A **327**, 517 (1979).
[23] Dimitri Kusnezov and W. E. Ormand, Phys. Rev. Lett. **90**, 042501 (2003).
[24] Srijit Bhattacharya *et al.*, Phys. Rev. C **77**, 024318 (2008).
[25] S. Mukhopadhayay *et al.*, Nucl. Instrum. Methods A **582**, 603 (2007).
[26] F. Puhlhofer, Nucl. Phys. A **280**, 267 (1977).
[27] A. V. Ignatyuk, G. N. Smirenkin, and A. S. Tishin, Sov. J. Nucl. Phys. **21**, 255 (1975) [Yad. Fiz. **21**, 485 (1975)].
[28] Y. Alhassid and N. Whelan, Nucl. Phys. A **565**, 427 (1993).
[29] W. D. Myers and W. J. Swiatecki, Nucl. Phys. **81**, 1 (1966).
[30] P. Moller and J. Nix, Nucl. Phys. A **361**, 117 (1981).
[31] K. T. R. Davies and J. R. Nix, Phys. Rev. C **14**, 1977 (1976).
[32] H. J. Krappe, J. R. Nix, and A. J. Sierk, Phys. Rev. C **20**, 992 (1979).
[33] P. Arumugam, G. Shanmugam, and S. K. Patra, Phys. Rev. C **69**, 054313 (2004).
[34] K. Neergard, Phys. Lett. B **110**, 7 (1982).
[35] Y. Alhassid and B. Bush, Phys. Rev. Lett. **65**, 2527 (1990).
[36] M. Kicihska-Habior *et al.*, Nucl. Phys. A **731**, 138 (2004).
[37] Masaaki Kimura and Hisashi Horiuchi, Phys. Rev. C **69**, 051304(R) (2004).